Available online at www.sciencedirect.com
SCIENCE DIRECT
Catalysis Today 107–108 (2005) 273–281
CATALYSIS TODAY
www.elsevier.com/locate/cattod

Hydroesterification and hydroformylation of 1-hexene catalyzed by rhodium complexes immobilized on poly(4-vinylpyridine)

Fernando Hung-Low [a], Gabriela C. Uzcátegui [a], Marisol C. Ortega [a], Angel B. Rivas [a], Jorge E. Yanez [a], Juan Alvarez [a], Alvaro J. Pardey [a,*], Clementina Longo [b]

[a] *Centro de Equilibrios en Solución, Escuela de Química, Facultad de Ciencias, Universidad Central de Venezuela, Caracas, Venezuela*
[b] *Centro de Investigación y Desarrollo de Radiofármacos, Facultad de Farmacia, Universidad Central de Venezuela, Caracas, Venezuela*

Available online 15 August 2005

Abstract

This work describes the catalytic hydroesterification and hydroformylation of 1-hexene by [Rh(cod)(amine)$_2$](PF$_6$) complexes (cod = 1,5-cyclooctadiene; amine = pyridine, 2-picoline, 3-picoline, 4-picoline, 3,5-lutidine or 2,6-lutidine) immobilized on poly(4-vinylpyridine) in contact with methanol under carbon monoxide atmosphere. In the presence of these immobilized complexes, 1-hexene, CO and methanol give methyl-heptanoate and 1,1-dimethoxy-heptane as the main reaction products and minor amounts of heptanal. The acetal by-product comes from the nucleophilic addition reaction of the methanol with the formed heptanal. Other products, such as H_2 and CO_2 coming from the catalysis of the water–gas shift reaction are observed. The reaction products distribution depends on the nature of the coordinated amine to the rhodium center and the reaction parameters.

Keywords: Hydroesterification; 1-Hexene; Rhodium catalyst; Carbon monoxide

1. Introduction

Reppe and Kröper performed the first synthesis of esters by reaction of an olefinic substrate with CO and alcohols (ROH) in the presence of transition metal complexes [1]. The hydroesterification reaction consists in the addition of a hydrogen atom and an alkoxycarbonyl group to an olefinic substrate (Eq. (1)) [2]. This reaction, also referred to as hydroalkoxycarbonylation or hydrocarbalkoxylation, has received considerable attention and it is the subject of a recent review by Kiss [3].

$$RHC{=}CH_2 + CO + ROH \rightarrow RH_2C{-}CH_2C(O){-}OR \quad (1)$$

Two catalytic cycles are proposed for the hydroesterification reaction [4]. One involves the formation of an alkoxycarbony–metal complex (M–COOR) [5–7]. The other, the hydroesterification reaction, involves the formation of an ester from alcoholysis of an intermediate metal acyl complex (M–C(O)–R) with a ROH group [8,9].

On the other hand, the hydroformylation of olefins using CO and H_2O involves the addition of a hydrogen atom and a formyl group to the carbon–carbon double bond (Eq. (2)). In this reaction, formation of metal hydride complex (M–H) and a further insertion of the coordinated olefin molecule in the M–H bond [10] generate an M–alkyl complex, which subsequently, inserts CO forming an acyl complex. Then, an in situ hydrogenolysis of the M–acyl complex forms an aldehyde [9].

$$RHC{=}CH_2 + 2CO + H_2O \rightarrow RH_2C{-}CH_2C(O){-}H + CO_2 \quad (2)$$

Studies in our laboratories have long been concerned with the use of the rhodium(I) complexes [Rh(cod)(amine)$_2$](PF$_6$) (cod = 1,5-cyclooctadiene; amine = pyridine, 2-picoline, 3-picoline, 4-picoline, 3,5-lutidine or 2,6-lutidine) immobilized on poly(4-vinylpyridine) as catalysts for the hydroformylation of 1-hexene under CO/H_2O [11,12],

* Corresponding author. Fax: +58 212 6051225.
E-mail address: apardey@strix.ciens.ucv.ve (A.J. Pardey).

0920-5861/$ – see front matter © 2005 Elsevier B.V. All rights reserved.
doi:10.1016/j.cattod.2005.07.081

water–gas shift reaction [13,14] and reduction of nitrobenzene under CO/H_2O [15], due to their easy preparation, good stability, high or moderate catalytic activities and the fine balance between electronic and steric effects induced by the methyl group on the pyridine ring of the metal coordinated amine. In addition, the immobilization of transition metal complexes into polymers combines the good activity, selectivity and reproducibility typical of homogeneous catalysts with the easy product separation and catalyst recovery characteristic of heterogeneous catalysts [16,17].

In order to expand our work on $Rh(amine)_2$/P(4-VP)-immobilized complexes, the present study reports the influence of the variations in reaction parameters on the catalytic hydroesterification and hydroformylation of 1-hexene in methanol by these complexes.

2. Experimental

2.1. Materials and instrumentation

Pyridine (py), methyl pyridines (2-picoline (2-pic), 3-picoline (3-pic) and 4-picoline (4-pic)) and dimethyl pyridines (3,5-lutidine (3,5-lut) and 2,6-lutidine (2,6-lut)) were obtained from Aldrich and distilled over KOH. Methanol, ethanol and 1-hexene (Aldrich) were distilled prior to use. Poly(4-vinylpyridine) (P(4-VP)) 2% cross-linked with divinylbenzene was used as provided by Reilly Industries. Water was doubly distilled. All gas mixtures He/H_2 (91.4%/8.6%, v/v), CO/CH_4 (95.8%/4.2%, v/v) and $CO/CH_4/CO_2/H_2$ (84.8%/5.1%/5.3%/4.8%, v/v) were purchased from BOC Gases and were used as received. The rhodium-immobilized complexes were synthesized as reported [13]. Analyses of Rh concentration in the filtered solution were performed on a Perkin-Elmer Lambda 10 UV–visible spectrophotometer and on a GBC Avanta atomic absorption spectrophotometer operated in the flame mode revealed that the immobilization of the rhodium complexes on 0.5 g of P(4-VP) is greater than 99%. These complexes will be referred as $Rh(amine)_2$/P(4-VP).

Gas samples analyses from catalysis and kinetics runs were performed as described in detail previously [13] on a Hewlett-Packard 5890 Series II programmable (ChemStation) gas chromatograph fitted with a thermal conductivity detector. The column employed was Carbosieve-B, 80–100 mesh obtained from Hewlett-Packard and using the He/H_2 mixture as the carrier gas. Analyses of liquid phase were done on a Hewlett-Packard 5890 Series II programmable gas chromatograph fitted with a HP-1 (methyl silicone gum, 50 m × 0.323 mm × 0.17 μm) column and flame ionization detector and using He as the carrier gas. A Varian Chrompack 3800 programmable gas chromatograph fitted with a CP-Sil-8-CB (phenyldimethylpolysiloxane) (30 m × 0.250 mm) column and a Varian Chrompack, Saturn 2000 mass selective detector were used to confirm the identity of the organic reaction products at the end of each run. Also the organic products were separated by column chromatography and analyzed by ^{13}C and ^{1}H NMR in a Jeol eclipse 270 NMR spectrometer.

2.2. Catalyst testing

Catalytic runs were carried out in all-glass reactor vessels consisting of a 100 mL round bottom flask connected to an "O" ring sealed joint to a two-way Rotoflow Teflon stopcock attached to the vacuum line. In a typical run, 0.5 g of the catalyst, 1.24 mL (1×10^{-2} mol) of 1-hexene and 10 mL of methanol (0.24 moles) were added to the glass reactor vessel, and then, the mixture was degassed by three freeze–pump–thaw cycles. The reaction vessel was charged with CO/CH_4 mixture at the desired CO partial pressure (0.7 atm at 25 °C, but 0.9 atm at 100 °C) and then, suspended in a circulating thermostated glycerol oil bath set at 100 °C for 5 h. The specified temperature was maintained at ±0.5 °C by continuously stirring the oil bath as well as the reaction mixture, which was provided with a Teflon-coated magnetic stirring bar. At the end of the reaction time, gas samples (1.0 mL) were taken by a gas tight syringe from the gaseous phase above the mixture and analyzed by GC. Also, liquid samples were removed and analyzed by GC and GC–MS. The CH_4 was used as internal standard to allow calculation of absolute quantities of CO consumed and H_2 and CO_2 produced. In addition, calibration curves were prepared periodically for CO, CH_4, H_2 and CO_2 and analyzing known mixtures checked their validities. The amounts of organic products were determined by using the response factor method for gas chromatographic analyses [18].

Catalytic runs under supra-atmospheric pressures were carried out in a 150 mL mechanically stirred stainless steel Parr autoclave charged with a 0.5 g of the catalyst, variable amounts of 1-hexene and 10 mL of methanol and pressurized with CO (10–38 atm at 130 °C). The autoclave was placed in a temperature-controlled heating device at (110–150) ± 1 °C and mechanically stirred for a given time. These pressures and temperatures were chosen as an average from previously reported systems [19]. At the end of the reaction time, gas and liquid samples were taken and analyzed by GC and GC–MS.

3. Results and discussion

3.1. General

The $Rh(amine)_2$/P(4-VP) catalysts were investigated as precursors for the catalytic 1-hexene/CO reactions in methanol. These catalytic systems are active for both, 1-hexene hydroesterification (Eq. (3)) and hydroformylation (Eq. (4)), the water–gas shift reaction (WGSR, Eq. (4)) and the acetalization of the formed heptanal with methanol (Eq. (6)). The relative extent of the competitive catalytic

Table 1
WGSR, hydroesterification and hydroformylation of 1-hexene in methanol, catalyzed by Rh(amine)$_2$/P(4-VP) complexes[a]

Amine (pK_a)[b]	Total [CO_2] mol × 10^{-4}	Total TF(CO_2)[c]	[H_2] mol × 10^{-4}	TF(H_2)[c]	[MH][d] mol × 10^{-4}	TF(MH)[c,d]	[Heptanal] mol × 10^{-4}	[1,1-DMH][e] mol × 10^{-4}
Pyridine (5.27)	5.8	28	1.7	8	2.7	13	0.2	4.2
3-Picoline (5.52)	10.2	49	1.9	9	4.4	21	0.2	8.4
2-Picoline (5.97)	9.0	43	1.5	7	5.2	25	0.1	7.3
4-Picoline (6.00)	10.0	48	2.9	14	12.1	58	0.1	7.3
3,5-Lutidine (6.63)	9.0	43	2.1	10	10.2	49	0.1	6.9
2,6-Lutidine (6.75)	3.3	16	1.0	5	8.1	39	0.1	2.1

[a] [Rh] = 1.9 wt.% (1×10^{-4} mol), 0.5 g of P(4-VP), [1-hexene] = 1.24 mL (1×10^{-2} mol), 1-hexene/Rh = 100, 10 mL (0.24 mol) of methanol, P(CO) = 0.9 atm at 100 °C for 5 h.
[b] From Ref. [20].
[c] TF(product) = [(mol of product)/(mol of Rh) × (rt)] × 24 h, where rt is reaction time in hours. Experimental uncertainty < 10%.
[d] MH, methyl-heptanoate.
[e] DMH, dimethoxy-heptane.

reactions can be established by comparing the amounts of the products. The results are shown in Table 1. All the mixtures left after cooling the reactor are separated into two phases. The upper liquid phase is pale-yellow and the solid phase has a brown color. Control experiments reveal that the activity toward the hydroesterification and hydroformylation of 1-hexene under CO was not observed when the mixtures of methanol with 1-hexene were tested under similar experimental conditions in the absence of any of the Rh(amine)$_2$/P(4-VP) catalysts.

Furthermore, we recently reported [21] that the same Rh(amine)$_2$/P(4-VP) in contact with sole water (P(CO) = 0.9 atm at 100 °C for 5 h) catalyzed the hydrocarboxylation of 1-hexene to heptanoic acid and the WGSR. Heptanal formation was not observed:

$$CH_3-(CH_2)_3-CH=CH_2 + CO + CH_3OH \xrightarrow{Rh/P(4\text{-}VP)} CH_3-(CH_2)_5-C(O)OCH_3 \quad (3)$$

$$CH_3-(CH_2)_3-CH=CH_2 + 2CO + H_2O \xrightarrow{Rh/P(4\text{-}VP)} CH_3-(CH_2)_5-C(O)H + CO_2 \quad (4)$$

$$CO + H_2O \overset{Rh/P(4\text{-}VP)}{\rightleftarrows} CO_2 + H_2 \quad (5)$$

$$CH_3-(CH_2)_5-C(O)H + 2CH_3OH \rightarrow CH_3-(CH_2)_5-C(OCH_3)_2H + H_2O \quad (6)$$

3.2. Hydroesterification and hydroformylation catalysis

Table 1 summarizes the results of the catalytic hydroesterification and hydroformylation of 1-hexene by the [Rh(cod)(amine)$_2$](PF_6) complexes immobilized on poly(4-vinylpyridine) in contact with methanol under CO atmosphere. GC and GC–mass analyses of the liquid phase runs allowed the identification of methyl-heptanoate, heptanal and 1,1-dimethoxy-heptane coming from the 1-hexene hydroesterification in methanol (Eq. (3)), hydroformylation (Eq. (4)) and the nucleophilic addition between methanol and the formed heptanal (Eq. (6)), respectively [22].

The results in methanol show that TF(methyl-heptanoate)/24 h (TF(MH/24 h) values depend on the nature of the coordinated amine and decrease in the following order: 4-picoline > 3,5-lutidine > 2,6-lutidine > 2-picoline > 3-picoline > pyridine.

3.3. WGSR catalysis

All of these Rh(amine)$_2$/P(4-VP) complexes, are also active for the catalysis of the WGSR under the conditions required for the catalytic hydroesterification of 1-hexene. GC analyses of the gas phase of the catalytic runs allowed the identification of H_2 and CO_2 as sole gaseous products. The H_2 and certain amount of CO_2 come from the WGSR. Another portion of the CO_2 produced comes from catalytic hydroformylation of 1-hexene under CO/H_2O (Eq. (4)) and the total CO_2 mass balances both (Eqs. (4) and (5)).

Catalytic WGSR is a known side reaction in hydroesterification [23–25]. Even though reagents and solvents used were pre-dried, formation of water via acetal formation was observed (Eq. (6)). Further, a control experiment shows no WGSR activity in the absence of the Rh(amine)$_2$/P(4-VP) catalysts under similar reaction conditions.

The results in methanol show that TF(H_2) values depend on the nature of the coordinated amine and decrease in the following order: 4-picoline > 3,5-lutidine > 3-picoline > pyridine > 2-picoline > 2,6-lutidine. These results are close to the reported for the catalytic WGSR by Rh(amine)$_2$/P(4-VP) complexes ([Rh] = 1×10^{-4} mol) in contact with 10 mL of 80% aqueous 2-ethoxiethanol under P(CO) = 0.9 atm at 100 °C [13], where the same tendency is observed.

The results show the positive effect of amine basicity on the WGSR, which increases with increasing pK_a of the amine ligand in absence of steric effect (present in the 2-picoline and 2,6-lutidine); namely, 4-picoline displays the highest activity. However, WGS reaction rates decrease sharply with increasing steric hindrance of the coordinated amine as shown by the lower activity of 2,6-lutidine and

Table 2
Recycling efficiency of WGSR, hydroesterification and hydroformylation of 1-hexene in methanol, catalyzed by Rh(4-pic)$_2$/P(4-VP)complex[a]

Used time	Total [CO_2] mol × 10^{-4}	Total TF(CO_2)[b]	[H_2] mol × 10^{-4}	TF(H_2)[b]	[MH][c] mol × 10^{-4}	TF(MH)[b,c]	[Heptanal] mol × 10^{-4}	[1,1-DMH][d] mol × 10^{-4}
1st	10.0	48	2.9	14	12.1	58	0.1	7.3
2nd	12.1	58	2.7	13	10.8	52	0.1	8.2
3rd	12.7	61	1.9	9	9.6	46	0.1	9.0
4th	16.3	78	2.5	12	6.0	29	0.1	10.3
5th	16.5	79	2.1	10	6.7	32	0.1	10.5

[a] [Rh] = 1.9 wt.% (1×10^{-4} mol), 0.5 g of P(4-VP), [1-hexene] = 1.24 mL (1×10^{-2} mol), 1-hexene/Rh = 100, 10 mL (0.24 mol) of methanol, P(CO) = 0.9 atm at 100 °C for 5 h.
[b] TF(product) = [(mol of product)/(mol of Rh) × (rt)] × 24 h, where rt is reaction time in hours. Experimental uncertainty < 10%.
[c] MH, methyl-heptanoate.
[d] DMH, dimethoxy-heptane.

these results suggest the presence of a critical steric parameter, which can be viewed as the effect of competition for binding to the catalytic center, which is more affected by steric constraints than by electronic effects. For example, the effective blockage of methyl groups in *ortho* position to nitrogen atom of the aromatic ring can prevent or decrease the rate of other elementary reactions of the catalytic cycle, which require a vacant coordination site on the metal center. This kind of blocking has been illustrated on the solid state isomerism and intermetallic interactions in the square planar rhodium(I), [RhX(CO)$_2$(amine)] (X = Cl, Br; amine = 2-picoline, 2,6-lutidine, etc.) complexes, that can be rationalized in terms of the steric hindrance of the amino ligand, which effectively prevent interactions between adjacent Rh(I) centers. The methyl group of these ligands when coordinated to the metal ion effectively blocks the axial position of the square planar environment. For example, complexes in which the amine ligand has a highly hindered N-donor atom are obtained in the non-stack form, while the stacked form is common for non-hindered ligands [26].

3.4. Acetal formation

Methanol adds to the carbonyl group of the catalytic formed heptanal (CH_3–$(CH_2)_5$–C(O)H) to yield the acetal 1,1-dimethoxy-heptane (CH_3–$(CH_2)_5$–$C(OCH_3)_2$H) (Eq. (6)).

Control experiments in the absence of the immobilized catalysts showed formation of 1,1-dimethoxy-heptane when a 1.0 mL of heptanal is placed in contact with 10 mL of methanol under P(CO) = 0.9 atm at 100 °C by 5 h. The heptanal conversion under the above-described conditions is 57%. Accordingly, Table 1 does not record the TF of acetal production due to its stoichiometric formation. However, in the presence of the immobilized Rh(4-pic)$_2$/P(4-VP) ([Rh] = 1.9 wt.%) complex, the catalytic formation of 1,1-dimethoxy-heptane is observed when a 1.0 mL of heptanal is placed in contact with 10 mL of methanol under P(CO) = 0.9 atm at 100 °C by 5 h. The heptanal conversion under the above-described conditions slightly increases from 57 to 65%. On the other hand, attempts to measure the catalytic impact on the production of these acetals by the others Rh-immobilized complexes were not made.

3.5. Recycling efficiency of the immobilized hydroxycarbonylation catalyst

The following studies were restricted to the most active Rh(4-pic)$_2$/P(4-VP) system. In order to check the leaching and recycling efficiency of the polymer-immobilized catalyst, two experiments were carried out. First, the solution remaining after a catalytic run was analyzed by UV–vis and by atomic absorption spectrophotometry techniques and less than 0.1% of rhodium was detected in this solution indicating absence of leaching. Second, the recycling efficiency was examined by re-using five consecutive times the same immobilized catalyst and these results are shown in Table 2.

Table 3
Carbon monoxide pressure effects on WGSR, hydroesterification and hydroformylation of 1-hexene in methanol, catalyzed by Rh(4-pic)$_2$/P(4-VP) complex[a]

P(CO) (atm)	Total [CO_2] mol × 10^{-4}	Total TF(CO_2)[b]	[H_2] mol × 10^{-4}	TF(H_2)[b]	[MH][c] mol × 10^{-4}	TF(MH)[b,c]	[Heptanal] mol × 10^{-4}	[1,1-DMH][d] mol × 10^{-4}
10	9.8	47	6.3	30	13.1	63	0.3	3.6
15	17.3	82	8.3	40	13.8	66	0.4	8.8
20	26.9	129	11.0	53	14.3	69	0.4	15.2
28	23.5	112	13.1	63	13.6	65	0.3	9.8
38	22.1	105	15.2	73	12.9	62	0.2	6.3

[a] [Rh] = 1.9 wt.% (1×10^{-4} mol), 0.5 g of P(4-VP), [1-hexene] = 1.24 mL (1×10^{-2} mol), 1-hexene/Rh = 100, 10 mL (0.24 mol) of methanol, 130 °C for 5 h.
[b] TF(product) = [(mol of product)/(mol of Rh) × (rt)] × 24 h, where rt is reaction time in hours. Experimental uncertainty < 10%.
[c] MH, methyl-heptanoate.
[d] DMH, dimethoxy-heptane.

Table 4
Temperature effects on WGSR, hydroesterification and hydroformylation of 1-hexene in methanol, catalyzed by Rh(4-pic)$_2$/P(4-VP) complex[a]

T (°C)	Total [CO_2] mol × 10^{-4}	Total TF(CO_2)[b]	[H_2] mol × 10^{-4}	TF(H_2)[b]	[MH][c] mol × 10^{-4}	TF(MH)[b,c]	[Heptanal] mol × 10^{-4}	[1,1-DMH][d] mol × 10^{-4}
110	9.0	43	5.2	25	14.3	69	1.0	3.3
120	13.1	63	7.5	36	10.8	52	0.7	4.6
130	26.9	129	11.0	53	8.7	42	0.4	15.2
140	37.1	179	19.6	94	7.7	37	0.2	17.1
150	64.4	309	41.9	201	7.1	34	0.1	22.9

[a] [Rh] = 1.9 wt.% (1×10^{-4} mol), 0.5 g of P(4-VP), [1-hexene] = 1.24 mL (1×10^{-2} mol), 1-hexene/Rh = 100, 10 mL (0.24 mol) of methanol, P(CO) = 20 atm for 5 h.
[b] TF(product) = [(mol of product)/(mol of Rh) × (rt)] × 24 h, where rt is reaction time in hours. Experimental uncertainty < 10%.
[c] MH, methyl-heptanoate.
[d] DMH, dimethoxy-heptane.

A change of TF values of the CO_2 and methyl-heptanoate were observed after five uses; for example, the TF(MH) value decreases from 58 to 29 (24 h^{-1}) and the amount of 1,1-dimethoxy-heptane increases from 7.3×10^{-4} to 10.5×10^{-4} mol. On the other hand, the total TF(CO_2), increases from 48 to 79 (24 h^{-1}). As stated before, the production of CO_2 is related to both, the WGSR (Eq. (5)) and hydroformylation of 1-hexene to heptanal (Eq. (4)). Because the TF(H_2) values do not change significantly, after repetitive use of the catalytic solid, it can be concluded that there is a significant increase of the heptanal formation, hence increasing the acetal production (Eq. (6)), as it is reflected by the amount of 1,1-dimethoxy-heptane. Apparently, there is an unknown change in the structure of the catalyst that favors heptanal formation, after repetitive uses. However, the system reaches constant TF values after the fourth to fifth use.

3.6. Catalysis activity in response to variation of P(CO), temperature and 1-hexene/Rh molar ratio

The effect of varying the CO pressure for the most active Rh(4-pic)$_2$/P(4-VP) system in methanol is summarized in Table 3. The plots of TF(H_2) values versus P(CO) for [Rh] = 1.9 wt.% at 130 °C shown in Fig. 1, is almost linear, indicating that the reaction is first order in [CO] at this temperature in the 10–38 atm range. A similar behavior was observed in the catalysis of the WGSR by [Rh(cod)(4-pic)$_2$](PF$_6$) immobilized on poly(4-vinylpyridine) 2% cross-linked with divinylbenzene in contact with 80% aqueous 2-ethoxyethanol in the P(CO) 0.5–1.9 atm range at 100 and 120 °C [27].

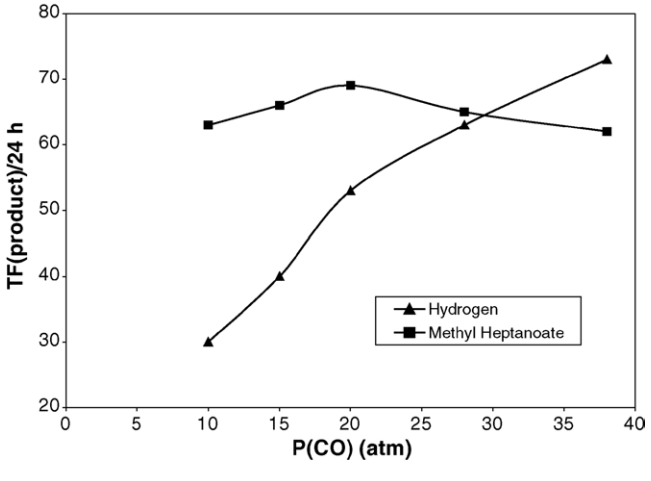

Fig. 1. A plot of TF(product)/24 h vs. P(CO): (▲) hydrogen and (■) methyl-heptanoate. *Reaction conditions:* [Rh] = 1.9 wt.% (1×10^{-4} mol), 0.5 g of P(4-VP), [1-hexene] = 1.24 mL (1×10^{-2} mol), 1-hexene/Rh = 100, 10 mL (0.24 mol) of methanol, 130 °C for 5 h. Lines drawn for illustrative purpose only.

This behavior suggests the formation of polymer anchored carbonyl–rhodium species followed by slower step to give H_2 and CO_2 (Eq. (7)):

$$\mathrm{P{-}[Rh]^+ + CO \xrightarrow{k_1} P{-}[Rh{-}CO]^+}$$
$$\mathrm{\xrightarrow{k_2, H_2O} P{-}[Rh]^+ + H_2 + CO_2} \quad (7)$$

$$\mathrm{P = P(4\text{-}VP)}$$

The WGSR rate law for such behavior would be:

$$\text{WGSR rate} = k_1 k_2 P(\mathrm{CO})[\mathrm{Rh}]_{\mathrm{tot}} \quad (8)$$

where $[Rh]_{tot}$ = P–$[Rh]^+$ + P–$[Rh–CO]^+$ and k_1 includes the solubility of CO in the medium and k_2 the $[H_2O]$. The above

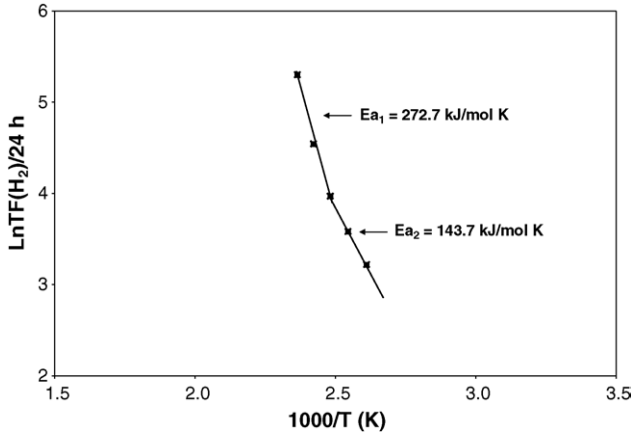

Fig. 2. The Arrhenius plot for WGSR catalysis. *Reaction conditions:* [Rh] = 1.9 wt.% (1×10^{-4} mol), 0.5 g of P(4-VP), [1-hexene] = 1.24 mL (1×10^{-2} mol), 1-hexene/Rh = 100, 10 mL (0.24 mol) of methanol P(CO) = 20 atm for 5 h.

expression (Eq. (8)) can be reduced to:

$$TF(H_2) = k_1 k_2 P(CO) \quad (9)$$

On the other hand, the activity of the hydroesterification reaction is not influenced by the variation of the $P(CO)$ in the 10–38 atm range at 130 °C (Fig. 1). This indicates that the formation of polymer-immobilized carbonyl–rhodium species is not the rate-determining step in the case of the catalytic hydroesterification of 1-hexene under carbon monoxide atmosphere.

Further, an increase in $P(CO)$ from 10 atm (Table 3) increases the production of 1,1-dimethoxy-heptane reaching a maximum at $P(CO) = 20$ atm. The production of 1,1-dimethoxy-heptane starts decreasing at $P(CO) > 20$ atm. These findings indicate the catalytic activity toward heptanal formation which leads to 1,1-dimethoxy-heptane production does not follow a linear dependence on $P(CO)$ in the range of 10–38 atm and suggest the formation of a less-active rhodium species at high CO pressure.

To determine the activation parameters for the WGSR, $TF(H_2)$/24 h values for the $Rh(4\text{-pic})_2$/P(4-VP) system were measured at various temperatures in the 110–150 °C range (Table 4). Fig. 2 displays the Ln $TF(H_2)$/24 h values against $1/T$ plot for [Rh] = 1.9 wt.%, [1-hexene] = 1×10^{-2} mol in 10 mL of methanol (0.24 mol) at $P(CO) = 20$ atm (under these conditions, the production of methyl-heptanoate reaches the highest value). The Arrhenius plot of Ln $TF(H_2)/(24\ h^{-1})$ values versus $1/T$ was non-linear in the 110–150 °C range, giving segmented curves. The apparent activation energies obtained from the slopes of the two segments are 143.7 kJ/(mol K) at temperatures < 130 °C and 272.7 kJ/(mol K) at temperatures > 130 °C. Arrhenius plots that are segmented indicate a change in the rate-limiting step between two competitive reactions [28]. Other factors, such as variation of nuclearity and/or oxidation state of catalytic active species may be responsible for curvatures in Arrhenius plots [14].

As shown in Table 4, varying of the temperature from 110 to 150 °C, increases the production of H_2, CO_2 and 1,1-dimethoxy-heptane and decrease the production of methyl-heptanoate. Similar tendencies for WGSR results were observed for the $[Rh(cod)(4\text{-pic})_2](PF_6)$-immobilized on poly(4-vinylpyridine) in carbon monoxide atmosphere (1 bar) in the 100–180 °C range under continuous-flow conditions [14].

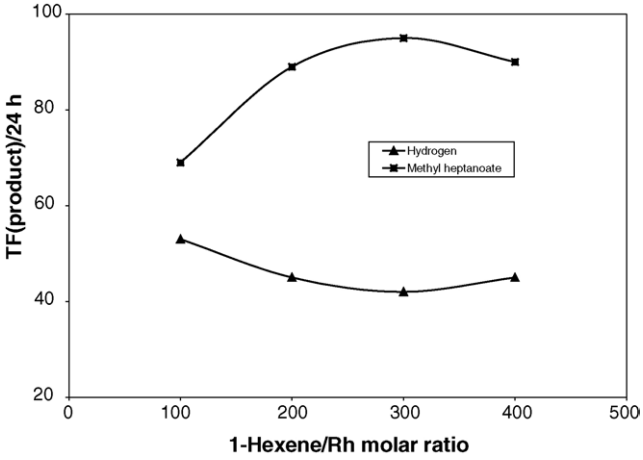

Fig. 3. A plot of TF(product)/24 h vs. 1-hexene/Rh molar ratio: (▲) hydrogen and (■) methyl-heptanoate. *Reaction conditions:* [Rh] = 1.9 wt.% (1×10^{-4} mol), 0.5 g of P(4-VP), 10 mL (0.24 mol) of methanol, 1-hexene = 1.24–4.96 mL, $P(CO) = 20$ atm at 110 °C for 5 h. Lines drawn for illustrative purpose only.

The effect of varying the 1-hexene concentration on the 1×10^{-2} to 4×10^{-2} mol range for the $Rh(4\text{-pic})_2$/P(4-VP) catalytic system is summarized in Table 5. The TF(MH) increases from 69 ($24\ h^{-1}$) ([1-hexene] = 1×10^{-2} mol), reaching a maximum value of 95 ($24\ h^{-1}$) at [1-hexene] = 3×10^{-2} mol and then, decreases to 90 ($24\ h^{-1}$) at [1-hexene] = 4×10^{-2} mol. As expected, the increase in the 1-hexene concentration favors the hydroesterification versus the WGSR and reaches a saturation point at high 1-hexene concentration. The plot of TF(MH)/24 h values versus [1-hexene]/Rh molar ratio under 20 atm of CO at 110 °C for 5 h shown in Fig. 3 indicates a reversible addition of 1-hexene to rhodium center on the 1-hexene/Rh (100–400) molar ratio range.

3.7. Mechanistic consideration

Scheme 1 illustrates a proposed mechanism for the WGSR and the hydroformylation and hydroesterification reaction of 1-hexene by the more active $Rh(4\text{-pic})_2$/P(4-VP)

Table 5
1-Hexene/Rh molar ratio effects on WGSR, hydroesterification and hydroformylation of 1-hexene in methanol, catalyzed by $Rh(4\text{-pic})_2$/P(4-VP) complex[a]

[1-Hexene] mol × 10^{-2} (1-hexene/Rh)	Total [CO_2] mol × 10^{-4}	Total $TF(CO_2)$[b]	[H_2] mol × 10^{-4}	$TF(H_2)$[b]	[MH][c] mol × 10^{-4}	TF(MH)[b,c]	[Heptanal] mol × 10^{-4}	[1,1-DMH][d] mol × 10^{-4}
1.0 (100)	27.1	130	11.0	53	14.3	69	0.4	15.2
2.0 (200)	18.5	89	9.4	45	18.6	89	0.6	8.5
3.0 (300)	18.1	90	8.8	42	19.7	95	0.6	8.9
4.0 (400)	26.5	127	9.4	45	18.8	90	0.5	16.3

[a] [Rh] = 1.9 wt.% (1×10^{-4} mol), 0.5 g of P(4-VP), 10 mL (0.24 mol) of methanol, 1-hexene = 1.24–4.96 mL, $P(CO) = 20$ atm at 110 °C for 5 h.
[b] TF(product) = [(mol of product)/(mol of Rh) × (rt)] × 24 h, where rt is reaction time in hours. Experimental uncertainty < 10%.
[c] MH, methyl-heptanoate.
[d] DMH, dimethoxy-heptane.

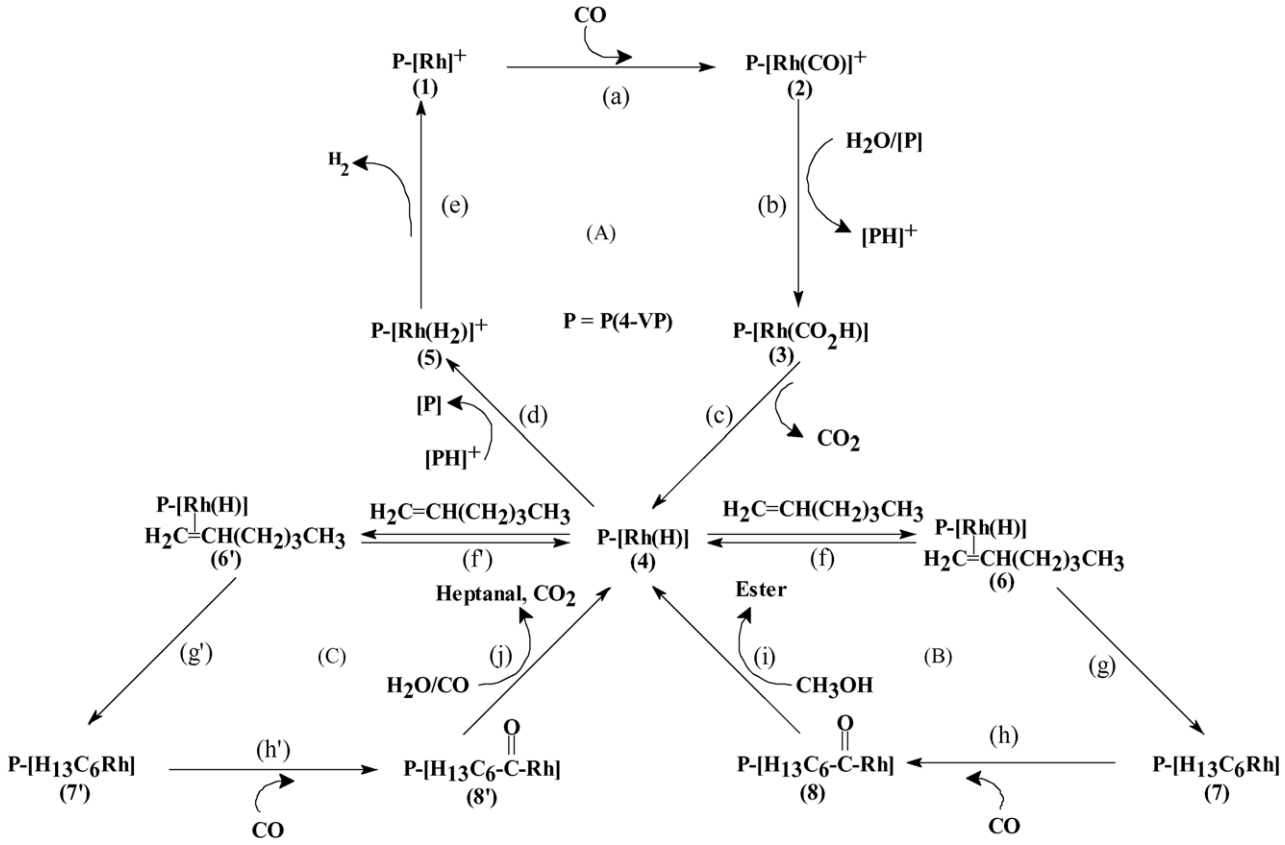

Scheme 1. Proposed mechanism.

system. The evaluation of the mechanism for H_2, CO_2, heptanal and methyl-heptanoate formation by the catalytic system based on Rh(4-pic)$_2$/P(4-VP) under CO shows a few key features: First, the early reported FT-IR, UV–vis reflectance, EPR and XPS and other studies on both Rh(4-pic)$_2$/P(4-VP) [14] and Rh(2-pic)$_2$/P(4-VP) solids [15] suggest the presence of mononuclear cationic Rh(I) and polynuclear anionic carbonyl Rh(-I) compounds as reaction intermediates in the WGSR and nitrobenzene reduction to aniline under CO, respectively, which probably are formed in the present system. Second, the CO_2 turnover frequencies in the presence of 1-hexene for the Rh(amine)$_2$/P(4-VP) systems are greater than the WGSR activity for the same system in the absence of 1-hexene. Presumably, in the former systems, a reactive intermediate prior to rate limiting H_2 formation is intercepted by catalytic species generated from 1-hexene addition to rhodium precursors. Third, the temperature studies also suggest mono-polynuclear equilibrium between active rhodium species, under the catalytic conditions. Fourth, the catalytic activity is first and zero order in P(CO) for the WGS and hydroesterification reaction, respectively, and optimal in the Rh(4-pic)$_2$/P(4-VP) system. Also, this catalytic system shows a reversible behavior in the 1-hexene addition. Fifth, a blank experiment using H_2/CO (synthesis gas) as an alternative to CO/H_2O was carried out in order to examine the possibility that molecular H_2 (coming from the WGSR) in presence of CO and 1-hexene forms heptanal under the catalytic conditions described in Tables 1–5. In this, a 0.5 g sample of Rh(4-pic)$_2$/P(4-VP) ([Rh] = 2 wt.%), 1.24 mL (1×10^{-2} mol) of 1-hexene and 10 mL of pre-dried 2-ethoxyethanol were added to a 150 mL glass reactor vessel, and then, the mixture was degassed by three freeze–pump–thaw cycles. The reaction vessel was charged with a CO/H_2 mixture ($P(H_2)$ = 0.9 and P(total) = 1.8 atm) at 100 °C for 5 h. GC and GC–mass analyses of the liquid phase revealed the presence of 2-hexene and 3-hexene as the only organic products, which come from the catalytic isomerization of 1-hexene. Consequently, the Rh(4-pic)$_2$/P(4-VP) system does not hydroformylate 1-hexene to heptanal under H_2/CO with these reaction conditions and these results strong suggest that the H_2 formed under the CO/H_2O system does not further react with 1-hexene. On the other hand, pre-dried 2-ethoxyethanol was used as medium system because it does not dehydrate as does methanol under the reaction conditions described above.

Given the above, the reaction mechanism depicted in Scheme 1 is proposed for WGSR, hydroesterification and hydroformylation of 1-hexene catalyzed by mononuclear cationic Rh(I) species. In Scheme 1, the amine ligands of the intermediate rhodium-immobilized complexes are omitted for clarity. Three connected cycles account for the observed products. In cycle (A), the formation of H_2 via WGSR implies coordination of CO to the immobilized P–[Rh]$^+$ (1)

complex (step a) to give the electrophilic P–$[Rh(CO)]^+$ specie (2). Nucleophilic attack by H_2O on the coordinated CO, perhaps assisted by free polymer (P) through its general base character, yields a hydroxycarbonylation complex P–$[Rh(CO_2H)]$ (3) and a protonated polymer $[PH]^+$ (step b). Elimination of CO_2 from the former complex gives the hydride P–[HRh] complex (4) (step c), which upon protonation by the pyridinium moiety $[PH]^+$ (step d) through its general acid character gives the dihydride complex P–$[Rh(H)_2]^+$ (5) and the free polymer. Reductive elimination of H_2 (step e) regenerates the starting P–$[Rh]^+$ complex (1) and closes the WGSR cycle [27].

Cycle (B) describes the formation of methyl-heptanoate (ester), which comes from in situ methanolysis of the Rh–acyl complex (8) (step i). The Rh–acyl complex arises from the reversible coordination of 1-hexene to form the intermediate complex (6) (step f). Insertion of the olefin to the Rh–H bond (step g) [10] gives P–$[C_6H_{13}Rh]$ (7). Then *cis*-migration of the C_6H_{13} group so formed to the P–[Rh–CO] moiety assisted by CO coordination (step h) gives the P–[Rh(acyl)] complex (8). Formation of the hydride–rhodium complex (4) (step i) closes the catalytic cycle (B).

Cycle (C) describes the formation of heptanal, which came from in situ hydrogenolysis of Rh–acyl complex (8′) (step j). Hydrogenolysis of the Rh–acyl intermediate, which leads to heptanal formation (step j), probably comes from *intra*-hydrogen transfer from Rh–H species formed under conditions similar to the WGSR (cycle A) [9,29]. Namely, nucleophilic attack by OH^- on a coordinated carbonyl ligand of the P–[Rh(CO)(acyl)] complex would afford the anionic rhodium hydroxycarbonyl P–$[Rh(CO_2H)(acyl)]^-$ complex and $[PH]^+$ (Eqs. (10) and (11)):

$$\mathrm{P{-}[Rh(CO)(acyl)] + H_2O \rightarrow P{-}[HRh(CO_2H)(acyl)]^- + H^+} \quad (10)$$

$$\mathrm{H^+ + P \rightarrow [PH]^+} \quad (11)$$

Decarboxylation of rhodium hydroxycarbonyl intermediate would generate a rhodium hydride complex P–$[HRh(acyl)]^-$ and CO_2 (Eq. (12)):

$$\mathrm{P{-}[Rh(CO_2H)(acyl)]^- \rightarrow P{-}[HRh(acyl)]^- + CO_2} \quad (12)$$

Reductive elimination of hydride–acyl complex produces the corresponding aldehyde and the coordinative unsaturated P–$[Rh]^-$ complex according to Eq. (13). The negative charge accumulated on the hydride–acyl complex favors the migration of coordinated H to Rh–C bond.

$$\mathrm{P{-}[HRh(acyl)]^- \rightarrow P{-}[Rh]^- + heptanal} \quad (13)$$

Protonation of the later anionic complex by $[PH]^+$ (Eq. (14) would give the starting P–[Rh(H)] complex (4) and the free polymer (P) to close the cycle (C).

$$\mathrm{P{-}[Rh]^- + [PH]^+ \rightarrow P{-}[Rh(H)] + P} \quad (14)$$

The overall reaction formation is shown in Eq. (15):

$$\mathrm{2CH_3{-}(CH_2)_3{-}CH{=}CH_2 + 4CO + CH_3OH + 2H_2O \rightarrow 2CO_2 + H_2 + CH_3{-}(CH_2)_5{-}C(O)OCH_3 + CH_3{-}(CH_2)_5{-}C(O)H} \quad (15)$$

Eq. (15) does not include the side product, 1,1-dimethoxy-heptane, which is principally formed in stoichiometric fashion.

In addition, the TF(MH) = 58 $(24\ h)^{-1}$ value, for the $Rh(4\text{-pic})_2$/(4-VP) system, is higher than the TF(heptanal) = 38 $(24\ h)^{-1}$ value, by a factor of 1.8. The calculated TF(heptanal) value reported here is based on total amount of CO_2 formed (Eqs. (4) and (5)) minus the amount of CO_2 (H_2) coming from the WGSR (TF = 10 $(24\ h)^{-1}$), keeping the CO_2/H_2 molar ratio equal to 1/1 according to Eq. (5). These results show, that the termination step by methanolysis of (8) affording methyl-heptanoate (step i) is faster than the termination step by hydrogenolysis of (8′) affording heptanal (step j), in spite that both products come from the same intermediate, namely the Rh–acyl complex (8 and 8′). On the other hand, methanol is in a much higher concentration than water. Accordingly, the methanolysis reaction is the rate-determining step.

Finally, the catalytic hydroesterification of 1-hexene by $Rh(4\text{-pic})_2$/(P/4-VP) system was also carried out in ethanol under the following reaction conditions: [Rh] = 1.9 wt.% (1×10^{-4} mol), 0.5 g of P(4-VP), [1-hexene] = 1.24 mL (1×10^{-2} mol), 1-hexene/Rh = 100, 10 mL (0.17 mol) of ethanol, P(CO) = 0.9 atm at 100 °C for 5 h. GC and GC–mass analyses of the liquid phase runs allowed the identification and quantification of ethyl-heptanoate (10.8×10^{-4} mol; TF = 52 $(24)^{-1}$), heptanal (0.1×10^{-4} mol) and 1,1-diethoxy-heptane (5.2×10^{-4} mol), arising from 1-hexene hydroesterification, hydroformylation and nucleophilic addition reaction between ethanol and formed heptanal, respectively. This system, also catalyzed the WGSR (TF(H_2) = 13 $(24)^{-1}$ and total TF(CO_2) = 37 $(24)^{-1}$. These results are almost similar to those observed for the $Rh(4\text{-pic})_2$/P(4-VP)/methanol system described above under similar reaction conditions. Accordingly, for the hydroesterification of 1-hexene by $Rh(4\text{-pic})_2$/P(4-VP) complex in contact with methanol or ethanol, carbon chain length of the aliphatic alcohols has little influence on the reaction rate in accordance with earlier reports [30–32]. Analyses of the effects of varying the nature of coordinated amine on the catalytic hydroesterification of 1-hexene in ethanol are still under study.

4. Conclusions

In this study, methyl-heptanoate and heptanal were synthesized by the hydroesterification and hydroformylation of 1-hexene. Both reactions were catalyzed by $[Rh(cod)(amine)_2](PF_6)$-immobilized poly(4-vinylpyridine) complexes

in contact with methanol under carbon monoxide atmosphere. Formation of the by-product 1,1-dimethoxy-heptane comes primarily from the nucleophilic addition reaction between methanol and catalytic formed heptanal. These Rh(amine)$_2$/P(4-VP) catalytic systems are active for the WGSR under the reaction conditions. The Rh(4-pic)$_2$/P(4-VP) system shows to be the most active among the amine-catalysts tested. On the other hand, reaction rates of the WGSR decrease markedly with the increase of steric hindrance on the coordinated amine. The increment of the *P*(CO) favors the WGSR activity while it disfavors the hydroesterification reaction.

Finally, a catalytic scheme for the production of H_2, CO_2, methyl-heptanoate and heptanal bearing common Rh–H catalytic species, is proposed.

Acknowledgments

This work was supported by CDCH-UCV (PG: 03.12.4957.2002) and FONACIT (S1-2002000260). The authors gratefully acknowledge support from CYTED: Red V-D and Project V-9. We thank Reilly Industries by donating the P(4-VP) (Lot No. 70515AA). We also thank Dr. Rodney P. Feazell (Baylor University) for helpful discussions.

References

[1] J.W. Reppe, H. Kröper, German Patent 765,969, 1953.
[2] P. Pino, F. Piacenti, M. Bianchi, in: I. Wender, P. Pino (Eds.), Organic Synthesis via Metal Carbonyls, vol. 2, John Wiley, NY, 1968.
[3] G. Kiss, Chem. Rev. 101 (2001) 3435.
[4] M. Kawana, S. Nakamura, E. Watanabe, H. Urata, J. Organomet. Chem. 542 (1997) 185.
[5] D. Milstein, Acc. Chem. Res. 21 (1988) 428.
[6] G. Cabinato, L. Toniolo, J. Organomet. Chem. 398 (1990) 187.
[7] T. Fuchikami, K. Ohishi, I. Ojima, J. Org. Chem. 48 (1983) 3803.
[8] J.P. Collman, L.S. Hegedus, Principles and Applications of Organotransition Metal Chemistry, University Science Books, Mill Valley, CA, 1980.
[9] P.C. Ford, A. Rockicki, Adv. Organomet. Chem. 28 (1988) 139.
[10] G. Consiglio, Chimia 55 (2001) 809.
[11] A.J. Pardey, J. Brito, M. Fernández, A.B. Rivas, M.C. Ortega, C. Longo, P.J. Baricelli, E. Lujano, S.A. Moya, React. Kinet. Catal. Lett. 74 (2001) 111.
[12] A.J. Pardey, J. Brito, A.B. Rivas, M.C. Ortega, C. Longo, P.J. Baricelli, E. Lujano, M. Yañez, C. Zuñiga, R. López, S.A. Moya, J. Chil. Chem. Soc. 48 (2003) 57.
[13] A.J. Pardey, M. Fernández, M. Canestrari, P. Baricelli, E. Lujano, C. Longo, R. Sartori, S.A. Moya, React. Kinet. Catal. Lett. 67 (1999) 325.
[14] A.J. Pardey, M. Fernández, J. Alvarez, C. Urbina, D. Moronta, V. Leon, M. Haukka, T.A. Pakkanen, Appl. Catal. A 199 (2000) 275.
[15] A.J. Pardey, M. Fernández, J. Alvarez, C. Urbina, D. Moronta, V. Leon, C. Longo, P. Baricelli, S.A. Moya, J. Mol. Catal. A 164 (2000) 225.
[16] F. Ciardelli, in: F. Ciardelli, T. Tsuchida, D. Wöhrle (Eds.), Macromolecular-Metal Complexes, Springer-Verlag, Berlin, 1996, p. 212.
[17] A.D. Pomogailo, Catalysis by Polymer-Immobilized Metal Complexes, English ed., Gordon and Breach Science Publishers, Singapore, 1998.
[18] H.M. McNair, J.M. Miller, Basic Gas Chromatography, Wiley-Interscience, NY, 1997 (Chapter 8).
[19] Yu.T. Vigranenko, S.Yu. Sukov, Russ. J. Appl. Chem. 72 (1999) 247.
[20] K. Schofield, Hetero-Aromatic Nitrogen Compounds, Plenum Press, NY, 1967 , pp. 146–148.
[21] F. Hung-Low, G.C. Uzcátegui, J. Alvarez, M.C. Ortega, A.J. Pardey, C. Longo, React. Kinet. Catal. Lett. 84 (2005) 87.
[22] R.T. Morrison, R.N. Boyd, Organic Chemistry, third ed., Allyn and Bacon, Boston, 1973 , p. 631.
[23] V.N. Zudin, V.D. Chinakov, V.M. Nyekipelow, V.A. Rogov, V.A. Likholobov, I. Yu. Yermakov, J. Mol. Catal. A 52 (1989) 27.
[24] A. Vavasori, L. Tonolio, J. Mol. Catal. A 110 (1996) 13.
[25] A. Seayad, A.A. Kelkar, R.V. Chaudhari, Ind. Eng. Chem. Res. 37 (1998) 2180.
[26] L.M. Vallarino, S.W. Sheargold, Inorg. Chim. Acta 36 (1979) 243.
[27] A.J. Pardey, M. Fernández, J. Alvarez, M.C. Ortega, M. Canestrari, C. Longo, P. Aguirre, S.A. Moya, E. Lujano, P.J. Baricelli, Bol. Soc. Chil. Quím. 45 (2000) 347.
[28] A.A. Frost, R.G. Pearson, Kinetics and Mechanism, Wiley, NY, 1961 , p. 24.
[29] P. Escaffre, A. Thorez, P. Kalck, J. Mol. Catal. 33 (1985) 87.
[30] J.F. Knifton, J. Org. Chem. 41 (1976) 2885.
[31] J.F. Knifton, J. Am. Oil Chem. Soc. 55 (1978) 496.
[32] G. Cavinato, L. Toniolo, J. Mol. Catal. A 104 (1996) 221.